Bistability in the sunspot cycle

Sumit Vashishtha*
Inria Lille

Katepalli R. Sreenivasan
New York University

–A direct dynamical test of the sunspot-cycle is carried out which indicates that a stochastically forced non-linear oscillator characterizes its dynamics. The sunspot series is then decomposed into its eigen time-delay coordinates. The analysis of these coordinates reveals that the sunspot series exhibits bistability, and suggests the possibility of modeling the solar cycle as a stochastically and periodically forced bistable oscillator, accounting for the Poloidal and Toroidal modes of the solar magnetic field. Such a representation of the sunspot series in terms of stochastic bistable dynamical system enables us to conjecture stochastic resonance as the key mechanism in amplifying the planetary influence of Jupiter on the sun, and that extreme events, due to turbulent convection noise inside the sun, dictate crucial phases of the sunspot cycle, such as the Maunder minimum.

INTRODUCTION

Solar cycle prediction, such as forecasting the amplitude and/or the epoch of an upcoming maximum, is of great importance for several reasons such as space weather, perhaps even earth's climate [1]. However, such predictions have been quite inconclusive owing to inherent fluctuations in the time period and amplitudes of each epoch of the solar cycle (Fig. 1). Even though the global aspects of the solar cycle are explained by the dynamo theory [2], the nature of the irregularities displayed by the sunspot time series is still being debated, and detailed understanding of its dynamics is far from complete.

Some past work [3, 4] has claimed evidence for the origin of the sunspot cycle in deterministic chaos, based on estimations of correlation dimension, Lyapunov exponents, and an increase of a prediction error with a prediction horizon. However, the dimension algorithms have been found to be unreliable [5, 6] when applied to relatively short experimental data, and properties consistent with stochastic processes (colored noises) such as autocorrelations can lead to spurious convergence of dimensional estimates; similar behavior has been observed for Lyapunov exponent estimators as well (REFERENCE?). Moreover, the increase of a prediction error with an increasing prediction horizon is not a property exclusive for chaos. Such behavior can also be observed in systems having a non-chaotic deterministic skeleton driven by a stochastic/noise component. The aim of this letter is to further investigate and characterize the role of noise and chaos in the sunspot cycle. Our point of departure is the so-called direct dynamical test [7–9] applied to the sunspot time series.

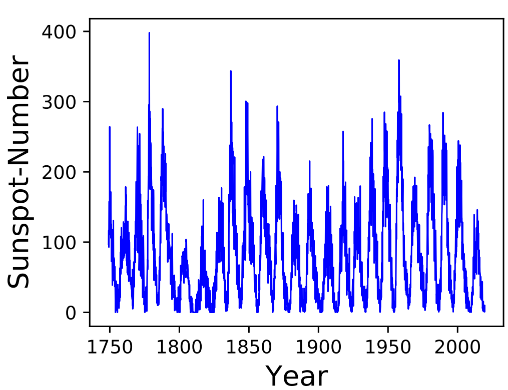

FIG. 1. Monthly mean sunspot numbers. The dynamics causing the observed irregularity of amplitude with dominant periodicity in the time series remains unknown.

DIRECT DYNAMICAL TEST

It has been challenging to differentiate between noise and low-dimensional chaos. Reference [8] developed an effective test for distinguishing one from the other. We carried out this test for the sunspot series in order to infer the underlying dynamics. The algorithm can be summarized as follows: From the monthly-mean sunspot time series $\{x(i)\}$, we first construct vectors $\{X_i\}$ by the time delay embedding technique [10]: $X_i = [x(i), x(i + L), ..., x(i + (m - 1)L)]$, with m as the embedding dimension and L as the delay time. Utilizing the findings in [4] in the context of the best values for delay time for the attractor reconstruction from the sunspot cycle, we choose L to be 10 in our computations. A value of 5 was used for m. We then compute the time-dependent exponent, $\lambda(t)$, as

$$\lambda(t) = \left\langle ln \left(\frac{\|X_{i+t} - X_{j+t}\|}{\|X_i - X_j\|} \right) \right\rangle \tag{1}$$

with $r \leq \|X_i - X_j\| \leq r + \Delta r$, where r and Δr are prescribed small distances. The angle brackets denote ensemble averages of all possible pairs of X_i and X_j. The integer t, called the evolution time, corresponds to time $t * dt$. Note that, geometrically, $(r, r + \Delta r)$ defines a shell, capturing the notion of scale. For clean chaotic systems, the $\lambda(t)$ curves first increase linearly with t until some predictable time scale, t_p, is reached, and flattens [9] thereafter. The linearly increasing parts of the $\lambda(t)$ curves corresponding to different shells collapse together to form an envelope for such clean systems. For noisy systems, the linearly increasing part of the $\lambda(t)$ curves, corresponding to small shells, break away from the envelope. The stronger the noise, the more $\lambda(t)$ curves break away from the envelope. Only if the noise is not strong enough to allow the linearly increasing parts of the $\lambda(t)$ curves, corresponding to some finite scale shells, to collapse together, can one say that the dynamics is chaotic. This property forms a direct dynamical test for deterministic chaos [8]. To illustrate this more clearly for the reader, we present a comparison of $\lambda(t)$ curves for the chaotic Lorenz-system and random noise in Fig. 2. Note that the linearly increasing parts of the curve collapse on each other for the Lorenz-system, whereas they break apart in the random noise case.

Note that, the $\lambda(t)$ plots give a qualitative picture of the dynamics. In order to infer quantitative aspects of the underlying dynamics one can evaluate the logarithmic displacement,

$$D(t) = ln \left\langle (\|X_{i+t} - X_{j+t}\|) \right\rangle = \lambda(t) + ln \left\langle (\|X_i - X_j\|) \right\rangle . \tag{2}$$

Next we carry out this analysis for the monthly-mean sunspot time-series. Fig. 3(a) shows the $\lambda(t)$ exponents (in the linearly increasing region) for four different shells, and Fig. 3(b) exhibits the $D(t)$ curves for the same shells. Some conclusions can be made; (a) Sunspot-series is not necessarily chaotic and the dynamics is greatly influenced by noise. This can be inferred from Fig. 3(a) as follows: If the time-series were to exhibit deterministic-chaos, all the plots should have collapsed over each other for the linearly increasing portion. This is not the case, thereby weakening the case for deterministic-chaos, and suggesting an important role of noise in the sunspots-dynamics. (b) Sunspot-series exhibits anomalous-diffusion [11]. This is exhibited in Fig 3(b), wherein the temporal-evolution of logarithmic displacement is plotted. Note that this displacement scales as t^α, where $\alpha = 0.218$, thus implying subdiffusion. Such a sub-diffusive scaling is observed in systems like stochastically-driven non-linear oscillators [12]. Overall, the direct-dynamical test shows that any possibility of chaos is overpowered by the effect of noise in the sunspot-series, and in a strict-sense, the sunspot-series doesn't exhibit deterministic-chaos, rather a stochastically driven non-linear oscillator best describes the evolution of the sunspot time-series. Observations supporting

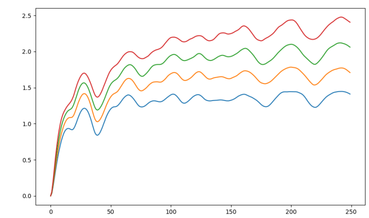

(a)

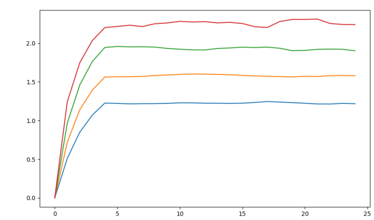

(b)

FIG. 2. Divergence exponents, $\lambda(t)$, for (a) time series for a chaotic solution of the Lorenz system; for (b) random noise time series. Note that the linearly increasing portion of the plots overlap for Lorenz system exhibiting deterministic chaos in (a), whereas the lines break apart in (b).

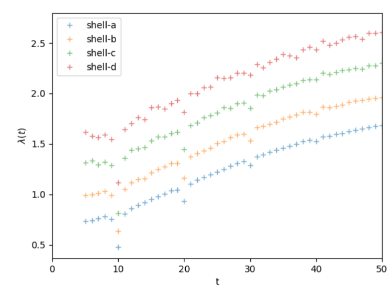

(a)

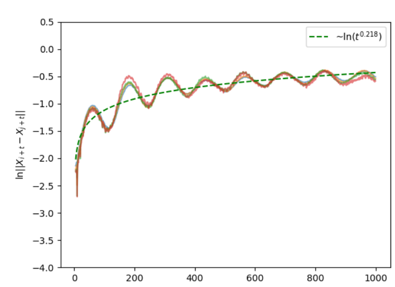

(b)

FIG. 3. (a) Divergence exponents, $\lambda(t)$, for the sunspot time-series in the linear-regime. Results for shells $(2^{-i/2}, 2^{-(i+1)/2})$, with $i = 7, 8, 9, 10$ are shown. Other shells have similar results. (b) Logarithmic displacement curves for the sunspot time-series. Note the sub-diffusive scaling for the curves.

the argument that a (randomly or otherwise) driven non-linear oscillator underlies the dynamics of the solar-cycle have been made in the past [13, 14] as well, however, as shown in [15], these relaxation-oscillator type models couldn't provide a complete description of the solar-cycle dynamics. A way to characterize this stochastic oscillator is to decompose the sunspot-series into its eigen-time-delay coordinates, inspired by Koopman operator theory, and we describe this next.

EIGEN-TIME-DELAY COORDINATES

Consider a dynamical system of the form,

$$\frac{\mathrm{d}}{\mathrm{d}t}\mathbf{x}(t) = \mathbf{f}(\mathbf{x}(t)), \tag{3}$$

the discretized form of which is given as,

$$\mathbf{x}_{k+1} = \mathbf{F}(\mathbf{x}_k) = \mathbf{x}_k + \int_{k\Delta t}^{(k+1)\Delta t} \mathbf{f}(\mathbf{x}(\tau))\mathrm{d}\tau, \tag{4}$$

Here $x(t) \in \mathbb{R}^n$ is the state of the system at time t and f represents the dynamic constraints that define the equations of motion. There are two major perspectives for analyzing such system; (a) The traditional geometric perspective of dynamical systems, which describes the topological organization of trajectories of $\mathbf{x}$, mediated by fixed points, periodic orbits, and attractors of the dynamics f; and (b) analyzing the evolution of measurements, $y = g(x)$, of the state. The later perspective was introduced by Koopman in 1931 [16–18]. The Koopman analysis relies on the existence of a linear operator $\mathcal{K}$ for the dynamical system in Eq. 4, and is given by,

$$\mathcal{K}g \stackrel{\Delta}{=} g \circ \mathbf{F} \quad \Rightarrow \quad \mathcal{K}g(\mathbf{x}_k) = g(\mathbf{x}_{k+1}). \tag{5}$$

The Koopman operator $\mathcal{K}$ induces a linear system on the space of all measurement functions g, and transforms the finite-dimensional nonlinear dynamics in Eq. 3 to an infinite-dimensional linear dynamics in 5, and provides a global linear representation, valid far away from fixed points and periodic orbits. Obtaining a finite-dimensional approximation of the Koopman operator is challenging, and a Koopman-invariant measurement system is key for such a realization. Eigen-time-delay coordiantes have been shown to approximate a Koopman-invariant measurement system, and have been used to construct best-fit linear models for various dynamical systems in the past [19, 20] using simple linear regression. These eigen-time-delay coordinates may be obtained from monthly mean sunspot number time series $\{x(t_1), x(t_2), x(t_3), \dots\}$, by taking a singular value decomposition of the Hankel matrix H,

$$\mathrm{H} = \begin{bmatrix} x(t_1) & x(t_2) & \dots & x(t_p) \\ x(t_2) & x(t_3) & \dots & x(t_{p+1}) \\ \vdots & \vdots & \ddots & \vdots \\ x(t_q) & x(t_{q+1}) & \dots & x(t_m) \end{bmatrix} = \mathrm{U}\Sigma\mathrm{V}^* \tag{6}$$

An important hyperparameter above is the number of delays q, which is chosen such that the delay duration $D = (q-1)\Delta t$ is large enough to capture a sufficient duration of the oscillation, where Δt is the sampling period. As a rule [21] of thumb, q should be chosen such that $D = T$, where T is the time period of the signal. We choose q such that D is slightly greater than 11 years, which is the average time-period for the sunspot-series. Eq. 6 yields a hierarchical decomposition of the matrix H into eigen-time-series given by the columns of U and V. These columns are ordered by their ability to express the variance in the columns and rows of the matrix H, respectively. The relative importance of each of these columns is expressed by the eigen-value diagonal matrix Σ containing σ_i^2.

Fig. 4a shows the eigen-value spectrum, which makes it clear that the dynamics underlying the solar-cycle is low-dimensional given that only the first 2-3 eigenvalues are significant. The columns of V provide a time series of the magnitude of each of the columns of UΣ in the data. The time-series for the columns of V corresponding to dominant eigenvalues, or the leading delay-coordinates, is shown in Fig. 4b. The first mode V_1, turns out to be an amplitude envelope of the original sunspot-series. The other two modes, besides having some phase lag, appear identical to each other. A careful look will convince one that these modes are essentially periodic-signals, with their amplitudes modulated by V_1. Fig. 5(a) shows the distribution of different values in the time-series of V_1. The bimodal nature of the histogram suggests bistability in the sunspot-series. These observations lead us to propose the following one-dimensional non-linear oscillator model for the sunspot-series,

$$\frac{dx}{dt} = -\frac{\partial U}{\partial x} + F(t) + \sum_i A_i \sin\omega_i t \tag{7}$$

where the first term on the right-hand side is the restoring force, with $U = -\alpha x^2 + \beta x^4$ as the quartic-potential function corresponding to a bistable-system. Along with a periodic external forcing, a random component $F(t)$ is also present. The nature of this noise-term (to first order) can be inferred by analyzing the time-derivative of the eigen-time-series V_1 (Eq. 7 without periodic forcing). The pdf of the derivative of this delay-coordinate is exhibited in Fig. 6(a). The same pdf is also shown on a scale where Gaussian-distribution is a straight line (probability-paper scale) in Fig. 6(b). The deviation from the straight line shows that the nature of noise-term driving the bistable-dynamics proposed above is

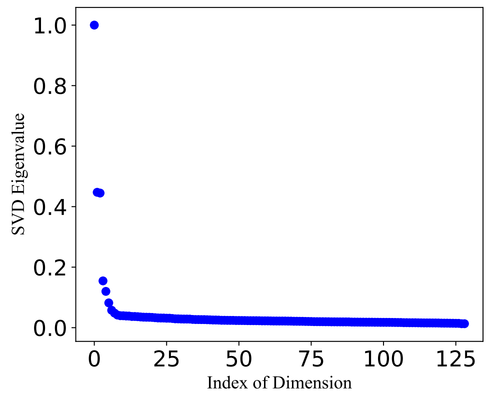

(a)

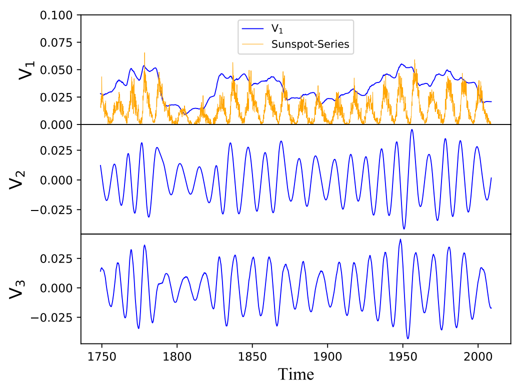

(b)

FIG. 4. (a) Distribution of the coordinate V_1. Note the bimodal nature of the distribution. This implies bistability and the possibility of the underlying dynamics being governed by a forced potential-well system; (b) The first three dominant delay-coordinates (V_1, V_2, V_3). Note that V_1 is amplitude envelope of the sunspot-series, whereas V_2 and V_3 are periodic signals with their amplitudes modulated by signal V_1

non-Gaussian and heavy-tailed. The bistable dynamics underlying the sunspot-series would account for the Poloidal and Toroidal components of the solar magnetic-field. Finally, note that Eq. 7 can also exhibit Stochastic Resonance, wherein a sub-threshold periodic signal can be entrained in the dynamics because of the additive role of noise. Fig. 5b shows the spectrum for the sunspot-cycle. Such a spectra, noise-background with peaks at drive frequencies and its harmonics, is characteristic for systems exhibiting Stochastic resonance [22]. The ratio of the eigenvalues corresponding to stochastic and periodic components in the present case is around 2.5, highlighting the weak contribution from the periodic-component of the forcing, and dominating role of the noise-term. Because of the limited amount of data for the sunspot-series, Standard analysis for stochastic resonance, such as residence-time-distribution, doesn't yield any meaningful information. That notwithstanding, if stochastic-resonance occurs in the above model for the sunspot-cycle, it could serve as a mechanism for amplification of weak planetary influences on the sun.

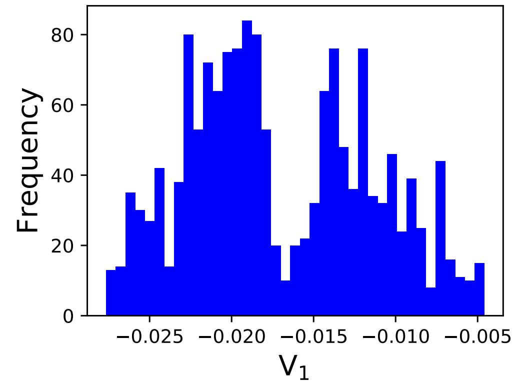

(a)

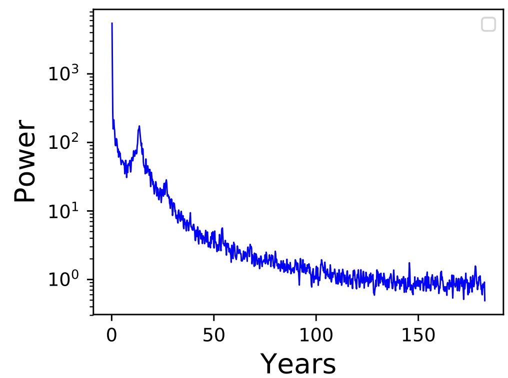

(b)

FIG. 5. (a) Distribution of the coordinate V_1. Note the bimodal nature of the distribution. This implies bistability and the possibility of the underlying dynamics being governed by a forced quartic-potential-well system; (b) Spectra of the sunspot-series.

PLANETARY INFLUENCE ON THE SOLAR CYCLE

There is a striking similarity between the average revolution time period of the Jupiter (around 11.86 years) and the (noisy) periodicity of the sunspot-cycle. Given this similarity, the possible role of (very-weak) planetary-forcing by Jupiter in influencing the solar magnetic-cycle cannot be ignored, and has been studied a bit in the past [23–26]. However, it is not clear how such weak planetary forcing could make itself so dominantly evdient in the solar-cycle. One possible mechanism is Stochastic-resonance [22], wherein a very weak external periodic signal is entrained in the dynamics at some optimal level of noise inside the system. A system exhibiting

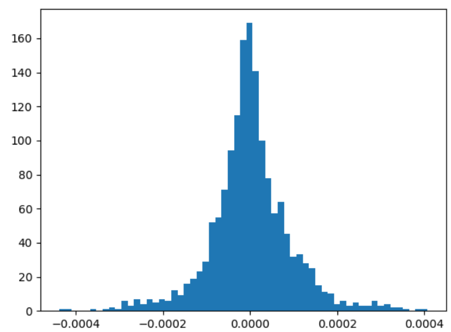

(a)

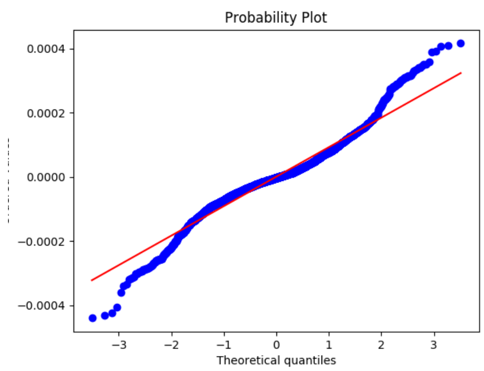

(b)

FIG. 6. (a) Distribution of the time-derivative of the eigen-delay-coordinate V_1; (b) Same distribution on a probability-paper scale

Stochastic resonance should typically be bistable, and bistability in the sunspot-series is what we reported in this paper. Thus, in light of our findings, stochastic resonance appears to be a plausible mechanism of how the weak-periodic planetary forcing from Jupiter could influence the solar-cycle, and this effect can be naturally incorporated in models of the type in Eq. 7. Note that the bistability reported in this paper would correspond to the poloidal and toroidal components of the solar magnetic-field. In fact, many state of the art models in solar-dynamo theory are based on transformations of the toroidal components to the poloidal components of the magnetic-field, and the other way around. See [27–29] for more details. Further note that, the noise in model 7 would ofcourse correspond to the noise of turbulent-convection in the sun.

MAUNDER-MINIMUM AS RARE EVENTS

We saw through Fig.6b that noise driving the bistable-dynamics is heavy-tailed in the sunspot cycle, and thus rare-events may play an important role in the evolution of the sunspot-cycle. Consider, for instance, Maunder minimum [30, 31], a phase of grand minima in the sunspot-cycle during 1645–1715, when the solar activity was strongly reduced. It has been established through an analysis of geological records that several Maunder minimum like periods have occurred in the past. It may well turn out that rare-events in the stochastic forcing, representing the extreme events in the turbulent convection, drive such phases. For instance, an extreme event can confine the dynamics to the potential well corresponding to Poloidal component of the magnetic field. This will result in significant reduction in the toroidal component (which directly corresponds to the number of sunspots(see [28])) of the magnetic field, and hence in the number of sunspots observed. A similar argument can be made to explain the phase where the values of maxima were very high in the sunspot cycle. Such rare event driven dynamics have been shown to play an important role in the dynamics of climate [32], transition to turbulence in turbulent-pipe-flows [33], and in aerodynamic bifurcations [34], among others.

CONCLUSIONS

We have shown that the sunspot-series exhibits bistability. First, a direct-dynamical test [8] of the sunspot-series indicated that a forced non-linear oscillator governs its dynamics. After that, an analysis of the dominant eigen-time-delay coordinates of the sunspot-series was carried out, and we concluded that the aforesaid oscillator is likely to be a one-dimensional bi-stable oscillator driven by heavy-tailed random forcing and weak periodic-forcing. Such a stochastic bistable dynamical system representation of the sunspot-series enabled us to conjecture stochastic resonance as the key mechanism in amplifying the planetary influence of Jupiter on the sun, and that rare-events in the turbulent-convection noise inside the sun could dictate crucial phases of the sunspot-cycle, such as the Maunder minimum. Our findings strongly encourage modeling attempts of the solar-cycle that incorporate the possibility of nonlinear effects such as stochastic resonance [35].

* sumit.vashishtha@inria.fr

[1] Kunihiko Kodera and Yuhji Kuroda. Dynamical response to the solar cycle. *J. Geophys. Res.*, 107(D24):ACL–5, 2002.
[2] Eric Ronald Priest. *Solar magnetohydrodynamics*, volume 21. Springer Science & Business Media, 2012.
[3] E Knobloch and AS Landsberg. A new model of the solar cycle. *Mon. Not. R. Astron Soc.*, 278(1):294–302, 1996.
[4] Michael D Mundt, W Bruce Maguire, and Robert RP Chase. Chaos in the sunspot cycle: Analysis and predic-

tion. *J. Geophys. Res.*, 96(A2):1705–1716, 1991.

[5] James Theiler. Spurious dimension from correlation algorithms applied to limited time-series data. *Phys. Rev. A*, 34(3):2427, 1986.

[6] M Dämmig and F Mitschke. Estimation of lyapunov exponents from time series: the stochastic case. *Phys. Lett. A*, 178(5-6):385–394, 1993.

[7] JB Gao, Sheng-Kwang Hwang, and JM Liu. When can noise induce chaos? *Phys. Rev. Lett.*, 82(6):1132, 1999.

[8] Jianbo Gao and Zhemin Zheng. Direct dynamical test for deterministic chaos and optimal embedding of a chaotic time series. *Phys. Rev. E*, 49(5):3807, 1994.

[9] JB Gao, Wen-wen Tung, and Nageswara Rao. Noise-induced hopf-bifurcation-type sequence and transition to chaos in the lorenz equations. *Phys. Rev. Lett.*, 89(25):254101, 2002.

[10] Norman H Packard, James P Crutchfield, J Doyne Farmer, and Robert S Shaw. Geometry from a time series. *Phys. Rev. Lett.*, 45(9):712, 1980.

[11] Alexander A Dubkov, Bernardo Spagnolo, and Vladimir V Uchaikin. Lévy flight superdiffusion: an introduction. *Int. J. Bifurcation Chaos*, 18(09):2649–2672, 2008.

[12] JB Gao, CC Chen, Sheng-Kwang Hwang, and JM Liu. Noise-induced chaos. *Int. J. Mod. Phys. B*, 13(28):3283–3305, 1999.

[13] M Paluš and Dagmar Novotna. Sunspot cycle: a driven nonlinear oscillator? *Phys. Rev. Lett.*, 83(17):3406, 1999.

[14] Pablo Daniel Mininni, Daniel Osvaldo Gomez, and GB Mindlin. Stochastic relaxation oscillator model for the solar cycle. *Phys. Rev. Lett.*, 85(25):5476, 2000.

[15] Yong Zou, Michael Small, Zonghua Liu, and Jürgen Kurths. Complex network approach to characterize the statistical features of the sunspot series. *New J. Phys.*, 16(1):013051, 2014.

[16] Bernard O Koopman. Hamiltonian systems and transformation in hilbert space. *Proc. Natl. Acad. Sci. USA*, 17(5):315, 1931.

[17] Igor Mezić. Analysis of fluid flows via spectral properties of the koopman operator. *Ann. Rev. Fluid Mech.*, 45:357–378, 2013.

[18] Igor Mezić. Spectral properties of dynamical systems, model reduction and decompositions. *Nonlinear Dynamics*, 41(1-3):309–325, 2005.

[19] J Nathan Kutz, Steven L Brunton, Bingni W Brunton, and Joshua L Proctor. *Dynamic mode decomposition: data-driven modeling of complex systems.* SIAM, 2016.

[20] Steven L Brunton, Bingni W Brunton, Joshua L Proctor, Eurika Kaiser, and J Nathan Kutz. Chaos as an intermittently forced linear system. *Nature communications*, 8(1):1–9, 2017.

[21] Kathleen P Champion, Steven L Brunton, and J Nathan Kutz. Discovery of nonlinear multiscale systems: Sampling strategies and embeddings. *SIAM J. App. Dyn. Sys.*, 18(1):312–333, 2019.

[22] Kurt Wiesenfeld and Frank Moss. Stochastic resonance and the benefits of noise: from ice ages to crayfish and squids. *Nature*, 373(6509):33–36, 1995.

[23] Frank Stefani, A Giesecke, N Weber, and T Weier. Synchronized helicity oscillations: A link between planetary tides and the solar cycle? *Solar Physics*, 291(8):2197–2212, 2016.

[24] Jose A Abreu, Jürg Beer, Antonio Ferriz-Mas, Kenneth G McCracken, and Friedhelm Steinhilber. Is there a planetary influence on solar activity? *A & A*, 548:A88, 2012.

[25] Dirk K Callebaut, Cornelis de Jager, and Silvia Duhau. The influence of planetary attractions on the solar tachocline. *Journal of atmospheric and solar-terrestrial physics*, 80:73–78, 2012.

[26] Ian RG Wilson, BD Carter, and IA Waite. Does a spin–orbit coupling between the sun and the jovian planets govern the solar cycle? *Publications of the Astronomical Society of Australia*, 25(2):85–93, 2008.

[27] S D'silva and AR Choudhuri. A theoretical model for tilts of bipolar magnetic regions. *Astron. Astrophys.*, 272:621, 1993.

[28] AR Choudhuri, M Schussler, and M Dikpati. The solar dynamo with meridional circulation. *Astro. Astrophys.*, 303:L29, 1995.

[29] Arnab Rai Choudhuri, Piyali Chatterjee, and Jie Jiang. Predicting solar cycle 24 with a solar dynamo model. *Phys. Rev. Lett.*, 98(13):131103, 2007.

[30] Douglas V Hoyt and Kenneth H Schatten. How well was the sun observed during the maunder minimum? *Solar Physics*, 165(1):181–192, 1996.

[31] JC Ribes and E Nesme-Ribes. The solar sunspot cycle in the maunder minimum ad1645 to ad1715. *A & A*, 276:549, 1993.

[32] Peter D Ditlevsen. Observation of α-stable noise induced millennial climate changes from an ice-core record. *Geophys. Res. Lett.*, 26(10):1441–1444, 1999.

[33] Dwight Barkley. Theoretical perspective on the route to turbulence in a pipe. *J. Fluid Mech*, 803(1), 2016.

[34] Ariane Gayout, Mickaël Bourgoin, and Nicolas Plihon. Rare event-triggered transitions in aerodynamic bifurcation. *arXiv preprint arXiv:2011.01063*, 2020.

[35] Carlo Albert, Antonio Ferriz-Mas, Filippo Gaia, and Simone Ulzega. Can stochastic resonance explain recurrence of grand minima? *The Astrophysical Journal Letters*, 916(2):L9, 2021.